Evolutionary game dynamics of combining the imitation and aspiration-driven update rules

Xianjia Wang,[1,2] Cuiling Gu,[2,*] Jinhua Zhao,[1] and Ji Quan[3]
[1]*Economics and Management School, Wuhan University, Wuhan 430072, China*
[2]*Institute of Systems Engineering, Wuhan University, Wuhan 430072, China*
[3]*School of Management, Wuhan University of Technology, Wuhan 430070, China*

(Received 14 March 2019; published 20 August 2019)

So far, most studies on evolutionary game dynamics in finite populations have concentrated on a single update rule. However, given the impacts of the environment and individual cognition, individuals may use different update rules to change their current strategies. In light of this, the current paper reports on a study that constructed a mixed stochastic evolutionary game dynamic by combining the imitation and aspiration-driven update processes. The target was to clarify the influences of the aspiration-driven process on the evolution of the level of cooperation by considering the behavior of a population in which individuals have two strategies available: cooperation and defection. Through a numerical analysis of unstructured populations and simulation analyses of structured populations and of the random-matching model, the following results were found. First, the mean fraction of cooperators varied alongside the probability with which the individual adopted the aspiration-driven update rule. In the Prisoner's Dilemma and coexistence games, the aspiration-driven update process promoted cooperation in the well-mixed population but inhibited it in structured ones and the random-matching model; however, in the coordination game, the aspiration-driven update process was seen to exert the opposite effect on cooperation by inhibiting the latter in a homogeneously mixed population but promoting it in structured ones and in the random-matching model. Second, the mean fraction of cooperators changed with the aspiration level in the differently structured populations and random-matching model, and there appeared a phase transition point. Third, the evolutionary characteristics of the mean fraction of cooperators maintained robustness in the differently structured populations and random-matching model. These results extend evolutionary game theory.

DOI: 10.1103/PhysRevE.100.022411

I. INTRODUCTION

In a biological sense, cooperative altruistic behavior, whereby individuals sacrifice their fitness to improve the fitness of other individuals, is common in nature. Cooperation among biological individuals increases the chances of the survival of the entire population. However, according to Darwin's theory of evolution, natural selection is based on competition and individuals selfishly maximizing their own interests. This theory, obviously, cannot explain ubiquitous cooperative behavior. Therefore, how unrelated and selfish individuals promote and maintain cooperative behavior has become a central issue in evolutionary biology. Evolutionary game theory [1–4], which is one of the key paradigms behind many scientific disciplines, from biology to behavioral sciences and the social economy, has been successfully applied to the study and explanation of the emergence of cooperation in competitive settings [5]. To date, many mechanisms have been proposed in the context of promoting competition in evolutionary game dynamics, such as kin selection [6], indirect reciprocity [7], direct reciprocity [8], multilevel selection [9], and network reciprocity [10–12]. Traditional evolutionary game theory was formulated for infinitely large populations, in which stochastic effects can be neglected and replication dynamics equations were generally used to describe the evolution of populations [2,13–15]. However, only in a few cases would a population [16] be large enough to justify the assumption of an infinite population. On the other hand, owing to nonlinearity, replication dynamic equations reveal very intricate dynamic processes. Therefore, compared to infinite populations, finite ones may have very significant differences, meaning that a stochastic approach is required to depict such differences [17–20].

Compared to the continuous representations of evolutionary dynamics in replicator equations, the stochastic evolutionary approach considers the state space of a system as discrete, and determines with certain probabilities the direction in which the system will evolve. Microscopic mechanisms (strategy update rules), in which individuals adopt to change their strategies in terms of various selection dynamics, are generally believed to play an important role in the evolution of cooperation in finite populations. Therefore, for a finite population, one of the most interesting open questions is how individuals would update their strategies according to the knowledge and conception of others and themselves. There have been several stochastic update processes, such as the Moran procedure [21–24], pairwise comparison [25], imitation [26–30], and aspiration-driven processes [31–36]. In the Moran process [24], at each time step an individual in a population is selected to produce a descendant proportional to its fitness, and the offspring replaces a randomly selected individual. In the imitation process, introduced by Szabó and Töke [4], an individual is randomly chosen and

*Gucui2020@whu.edu.cn

compares their payoff with that of a second randomly chosen individual, who is more likely to be imitated when the payoff for the second individual is higher. The aspiration-driven update rule is defined as follows: an individual will switch strategy if the current payoff is lower than the aspiration level; otherwise, the present strategy is maintained. Here, the aspiration level can be interpreted as the degree of satisfaction (preference) of the learning individual.

Many studies [16,37] have examined the Moran procedure, imitation, and aspiration-driven processes to explain cooperative behavior, but have mainly focused on a single update rule. Assuming that all individuals in a population would adopt the same updating rules is not realistic. Therefore, in order to study the evolution of cooperation, some studies have applied combinations of different update rules by grouping populations. For instance, to study the evolution of cooperation in different topologies via the mean-field equation, some studies have assumed [38] that certain individuals in a finite population would adopt the imitation rule, whereas the remaining individuals would adopt the innovation rule. Liu [39,40] divided a finite population into two groups with different strategy update rules and studied the evolution of cooperation through the fixation probability, fixation time, or mean abundance of the cooperators. Zhang [41] distributed populations into fast and slow groups, and then studied the population dynamics when interacting individuals differed in terms of the time scale of their updating processes. Despite meaningful progress, there are still some situations of great practical relevance that remain less explored. One of the problems here concerns the tendency—due to the influence of the environment and other factors—of individuals to change their strategies often according to two or more update rules, i.e., as a result of the influence of environmental factors and the complexity of their knowledge, individuals are likely to adopt several different updating rules, with different probabilities, to update their strategies. Wang [42] established a hybrid model based on the Moran and imitation processes to study how both updating rules influence evolutionary game dynamics. Moreover, in addition to the imitation update rule, an individual could change their current strategies according to the aspiration-driven process. For example, in general, an ant hunts for food by imitation, but sometimes uses its own experience instead [33,43]. This phenomenon also occurs in human society. In light of this, the current study established a new mixed model to study the influence of the two update processes, namely, the aspiration-driven and imitation rules, on cooperative evolution in different topologies.

Only cognitively capable individuals were studied, not irrational species, on the basis of the following aspect. In the real world, while there exists a population of individuals who alter their strategies by mimicking their better-off neighbors (those with higher incomes), sometimes, individuals change their present strategies in accordance with their own expectations (aspiration level) to decide whether to change strategies, regardless of the payoffs of a randomly chosen neighbor. Thus the current paper proposes a new mixed dynamic model in which an individual alters its previous strategy according to the imitation process with probability $1-\gamma$, ($\gamma \in [0, 1]$), and the aspiration-driven process with probability γ. The hybrid model was analyzed in both a homogeneous and structured

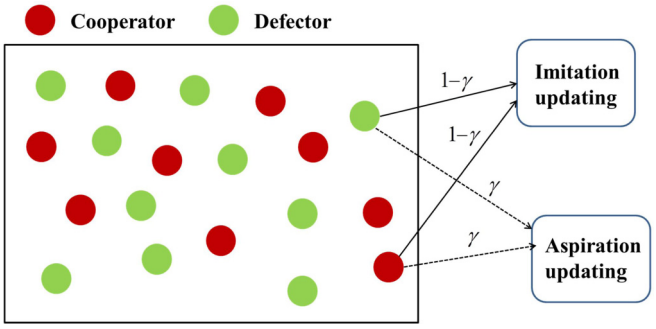

FIG. 1. In this neoteric mixed model, individuals play a symmetric 2×2 game in a finite well-mixed population. Each individual adopts the imitation rule to change strategy with the probability $1-\gamma$, and the aspiration rule with probability γ, where $\gamma \in [0, 1]$.

population. For sketches of the proposed mixed model in well-mixed finite population and square lattice network, see Fig. 1 and Fig. 2, respectively. In addition, based on the mixed model, the random matching model studied in Ref. [44–46] was also explored (see Fig. 3).

For irrational species, the change rate of the state of a population over time is analyzed based on replicator dynamics. However, for a finite population with cognitive capabilities, what matters is not the rate of change of the population but the limit state of the latter under the microscopic update mechanism. Therefore, the index of the mixed evolutionary game model is that of the mean fraction of cooperators (MFC) when the population reaches the equilibrium state. Clarifying the nature of the proposed mixed evolutionary dynamics, upon combining two updating processes, is the scope of this paper. The established model was analyzed by observing its performance in three general games (Prisoner's Dilemma, coexistence, and coordination) and using numerical and simulation analysis in the well-mixed and spatial structure populations, respectively.

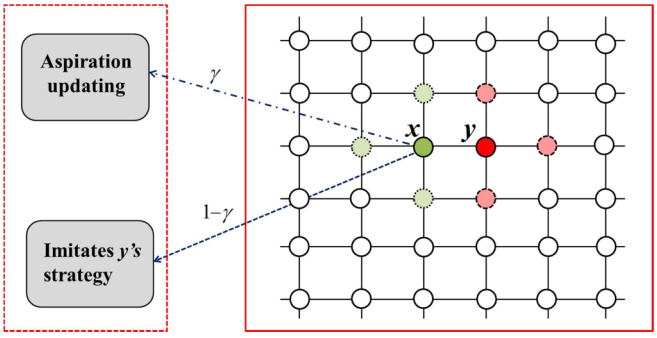

FIG. 2. Individuals located on a two-dimensional four-neighbor square lattice (in the red box on the right), in which randomly selected individual x, defined as the focal individual, interacts with its four neighbors. Individual x can mimic the strategy of one of its four neighbors (defined as the model individual, y) with probability $1-\gamma$ by comparing its current average payoffs, π_x, with its neighbor's average payoff, π_y, and adopt the aspiration update with probability γ, where $\gamma \in [0, 1]$, by comparing its current average payoffs with its own aspiration level.

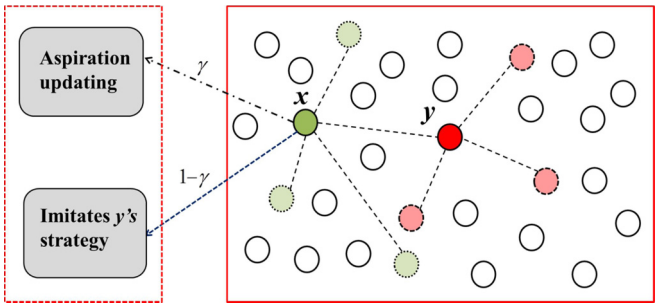

FIG. 3. The schematic diagram of the random matching model is here provided by taking $k = 4$ as an example. The modified sampling scheme in a well-mixed population of size N is shown in the red box on the right. The two competitors (green and red, respectively) both interact with each other, plus $k - 1 = 3$ random members (light green and light red, respectively) of the population. The red agent, x, and blue agent, y, are considered as the focal individual and the imitative individual, respectively. The update rules for focal individuals, x, are shown in the dashed red box on the left. The focal individual adopts the imitation rule to change its current strategy with the probability $1 - \gamma$ by comparing its current average payoffs, π_x, with the model individual's average payoff, π_y, and the aspiration-driven rule with probability γ, where $\gamma \in [0, 1]$, by comparing its current average payoffs with its own aspiration level, α.

The remainder of this paper is arranged as follows. Section II introduces three models: mixed models in the well-mixed and structured populations, and a random-matching model. Section III reports the theoretical and numeral analyses in the unstructured population, followed by the simulated analyses of the structural populations and the simulated analyses of the random matching model. Section IV presents the conclusion.

II. MODELS

Three models are detailed in this section: models in the well-mixed and structured populations, and the random matching model based on the imitation update process and aspiration-driven update process. In all of these models, individuals have two alternative strategies: C (cooperation) and D (defection). At each interaction, individuals gain a payoff according to a payoff matrix [47], which can be defined as

$$\begin{array}{c} \\ C \\ D \end{array}\begin{array}{c} \begin{array}{cc} C & D \end{array} \\ \begin{bmatrix} R & S \\ T & P \end{bmatrix} \end{array}. \tag{1}$$

Two cooperative individuals receive a reward, R, whereas two defectors receive a punishment, P. If a cooperator interacts with a defector, then the former receives S while the latter obtains a temptation, T.

This study considered the Prisoner's Dilemma game, in which strategy D always has a higher payoff ($T > R > P > S$) and is always dominant; the coexistence game, in which both strategies C and D receive the highest payoffs when interacting with the other respective strategy ($R < T, S > P$); and the coordination game, in which both strategies C and D receive the highest payoffs when interacting with their own types ($R > T, S < P$).

A. Well-mixed populations

In a well-mixed population of size N, at every discrete moment of time, t, the state of the population is described by the number of individuals, i, denoting the current number of cooperators. The average payoffs of individuals using strategies C and D are given by [48,49]

$$\pi_C = \frac{R(i-1) + S(N-i)}{N-1}, \tag{2a}$$

$$\pi_D = \frac{Ti + P(N-i-1)}{N-1}. \tag{2b}$$

We denote the fitness of the cooperators and defectors as f_A and f_B, respectively. Now, we use an exponential mapping [46]:

$$f_A = e^{\omega \pi_A}, \tag{3a}$$

$$f_B = e^{\omega \pi_B}. \tag{3b}$$

The parameter $\omega \geqslant 0$ represents the selection intensity, which plays a critical role in social learning and cultural evolution. If $\omega = 0$, the selection is neutral and we have an undirected random walk. If $0 < \omega \ll 1$, the selection is weak. The concept of weak selection was introduced by Nowak [21] and refers to the effects of small differences in the payoffs. When the selection intensity ω is large, the selection is strong. Selection intensity describes how selective bias and fluctuations influence each other.

In the imitation process [50], a random individual is selected and its payoff compared with that of another randomly selected individual. Generally, individuals imitate the strategy of a more successful peer. The state of the system can change by one (at most) at each time step; thus, the transition probabilities are defined as follows:

$$p_{i,i+1}|_{\text{imitation}} = \frac{N-i}{N}\frac{i}{N}\frac{1}{1+e^{-\omega(\pi_C-\pi_D)}}, \tag{4a}$$

$$p_{i,i-1}|_{\text{imitation}} = \frac{N-i}{N}\frac{i}{N}\frac{1}{1+e^{\omega(\pi_C-\pi_D)}}, \tag{4b}$$

$$p_{i,i}|_{\text{imitation}} = 1 - p_{i,i+1}|_{\text{imitation}} - p_{i,i-1}|_{\text{imitation}}. \tag{4c}$$

All other entries of the transition matrix are 0. In the absence of mutation, the imitation update process corresponds to a discrete Markov chain with a state space $\{0, 1, \cdots, N\}$, of which 0 and N represent absorbing states.

Unlike the imitation process, an aspiration-driven update does not require additional information about the strategic environment, and can be interpreted as being more spontaneous. In the latter process, individuals adjust their strategies by comparing the payoff of the game to that of the aspiration level α, which can be interpreted as the degree of individuals' satisfaction with the learning individual [51]. Thus, the transition probabilities [48] can be expressed as

$$p_{i,i+1}|_{\text{aspiration}} = \frac{N-i}{N}\frac{1}{1+e^{-\omega(\alpha-\pi_D)}}, \tag{5a}$$

$$p_{i,i-1}|_{\text{aspiration}} = \frac{i}{N}\frac{1}{1+e^{-\omega(\alpha-\pi_C)}}, \tag{5b}$$

$$p_{i,i}|_{\text{aspiration}} = 1 - p_{i,i+1}|_{\text{aspiration}} - p_{i,i-1}|_{\text{aspiration}}. \tag{5c}$$

All other entries of the transition matrix are 0. The aspiration-driven process is represented by a Markov chain, defined in a state space $\{0, 1, \cdots, N\}$ without absorbing states.

The aspiration level α influences the stochastic updating strategy [34,37] insofar as the individuals are more likely to switch strategy if their aspiration levels are not met. The probability of switching is random when an individual's payoffs are close to their level of aspiration, thereby reflecting the basic degree of uncertainty in the population. If the payoffs exceed an individual's aspiration, then strategy switching is impossible. When the aspiration level is higher than the payoff, the gap between aspiration and payoff grows wider and the probability of switching is higher. As the intensity, ω, increases, the importance of the impact of the difference between the payoff and aspiration level increases.

In the current proposed process, individuals change strategies by imitating others or by means of aspiration renewal. Let it be supposed that the probability of an individual's adoption of the imitation update rule is $1-\gamma$. Conversely, the probability of adopting the aspiration update rule is γ. The weighting coefficient, $\gamma \in [0, 1]$, represents the trade-off between the two update rules. In particular, to update their strategy, a player only adopts the imitation rule if $\gamma = 0$, and the aspiration-driven update rule if $\gamma = 1$. Figure 1 vividly illustrates this model. The spread of successful strategies is modeled by a birth–death process in discrete time. At each time step, the number of cooperators can increase/decrease by one, or stay the same. Therefore, the matrix of the transition probabilities of the Markov process in this proposed model is tri-diagonal, and can be expressed as follows:

$$p_{i,i+1} = (1-\gamma)\frac{i}{N}\frac{N-i}{N}\frac{1}{1+e^{\omega(\pi_D-\pi_C)}} + \gamma\frac{N-i}{N}\frac{1}{1+e^{\omega(\pi_D-\alpha)}}, \tag{6a}$$

$$p_{i,i-1} = (1-\gamma)\frac{i}{N}\frac{N-i}{N}\frac{1}{1+e^{\omega(\pi_D-\pi_C)}} + \gamma\frac{i}{N}\frac{1}{1+e^{\omega(\pi_C-\alpha)}}, \tag{6b}$$

$$p_{i,i} = 1 - p_{i,i+1} - p_{i,i-1}. \tag{6c}$$

All other entries of the transition matrix are 0, where i refers to the current number of cooperators and is used to express the state of then population. Even in a homogeneous population, there exists a probability that an individual could switch to another strategy as a result of dissatisfaction with a payoff–aspiration difference. In addition, the current paper considers the aspiration level to reflect the internal pursuit of an individual's ego, assuming that each individual hopes for higher returns. Without the introduction of mutation or random strategy exploration, the mixed dynamic process of a strategy can be described as a Markov process, with the state space $\Omega = \{i, i = 0, 1, 2, \cdots, N\}$.

B. Structured populations

In the structured populations (square lattice, small world, and scale-free networks), the nodes represent individuals and the links characterize the interactions among them. The players in structured populations can change strategies based on the imitation rule with the probability $1-\gamma$, and the aspiration-driven rule with the probability γ.

First, a player termed the focal individual, x, was randomly selected. This focal individual, x, collects the payoff from all of its direct k (k is the degree of the structured populations) neighbors around her. The average payoff of x can be defined as

$$\pi_x = \frac{1}{k}\sum_{y' \in \mathrm{H_x}} a_{xy'}, \tag{7}$$

where $\mathrm{H_x}$ is a set composed by the nearest k neighbors of focal individual x, and $a_{xy'}$ is x's payoff from the interaction between focal individual x and its one neighbor, y'. Subsequently, focal individual x randomly chose one neighbor, y, from $\mathrm{H_x}$ ($y \in \mathrm{H_x}$) as the model individual. The same steps were applied to obtain the mean payoff, π_y, of y.

Then, with the probability $1-\gamma$, the focus individual x compares its average payoff with that of its neighbor, y, to decide whether to change its current strategy. However, with the probability γ, the focus individual x compares its average payoff with its aspiration level, α, to decide whether to change its current strategy. Therefore, the probability of individual x changing its current strategy to the opposite one can be defined as

$$P_S = (1-\gamma)\frac{1}{1+e^{\omega(\pi_y-\pi_x)}} + \gamma\frac{1}{1+e^{\omega(\pi_x-\alpha)}}, \tag{8}$$

where the parameter $\omega \geqslant 0$ represents the selection intensity. Taking the square lattice as an example, Fig. 2 shows the mixed update model.

C. Random matching model

According to Refs. [45,46], a random-matching model represents a well-mixed analog to interactions on regular graphs with a degree of k, which scheme naturally implements the modified sampling scheme shown in the right-hand red box of Fig. 2. A random-matching model is now defined based on the mixed updating rules of combining the imitation process and the aspiration-driven updating rule.

In the current time step, two individuals are randomly selected, named focal individual x and model individual y, from a population of size N, where agents x and y are competitors. Then, from the rest $N-2$ individuals, $k-1$ individuals are randomly selected for each of x and y as the interacting neighbors. The focal individual, x, interacts with its $k-1$ interacting neighbors, and the respective payoffs of x are denoted by $a_{x,1}, a_{x,2}, \cdots, a_{x,k-1}$. In addition, x interacts with the model individual, y, and the payoff of x is denoted by a_{xy}. Thus, the average payoff of the focus individual x is

$$\pi_x = \frac{1}{k}\left(\sum_{s=1}^{k-1} a_{x,s} + a_{xy}\right). \tag{9}$$

Similar to the calculation of π_x, the average payoff, π_y of model individual y can be obtained.

Focal individual x changes its strategy based on the following rule (Fig. 3). The focal individual x adopted imitation update rule with a probability of $1-\gamma$ by comparing its average payoff π_x to that of individual y. If the payoff

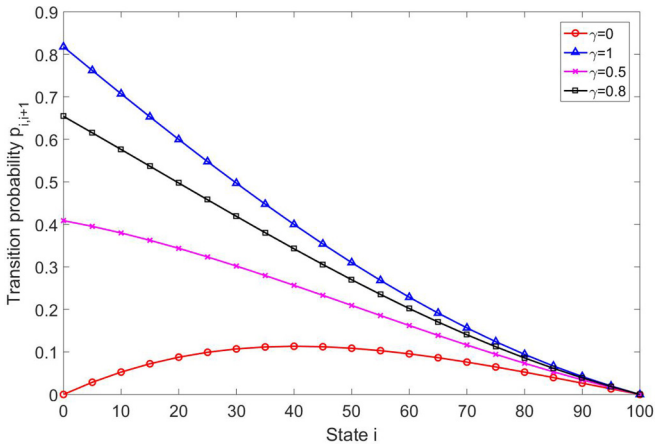

FIG. 4. Transition probabilities vary with state i in the Prisoner's Dilemma, where $R = 3$, $S = 1$, $T = 5$, $P = 2$, $\omega = 0.5$, and $\alpha = 4$. The red circles and blue triangles represent the respective transition probabilities, $p_{i,i+1}$, of the imitation and aspiration-driven update processes. The magenta crosses and black squares represent the respective transition probabilities, $p_{i,i+1}$, of the mixed evolutionary process with $\gamma = 0.5$ and $\gamma = 0.8$.

of the focal individual is greater than that of individual y, then the focal individual x does not change its current strategy; otherwise, the strategy changes. The focal individual x adopted aspiration-driven update rule with a probability of γ by comparing its average payoff π_x to its aspiration-level α. If the average payoff π_x is greater than its aspiration level α, then the individual x does not change its strategy to the opposite scenario. Therefore, the probability of the focal individual, x, changing its current strategy to the opposite one can be defined as

$$P_R = (1-\gamma)\frac{1}{1+e^{\omega(\pi_y-\pi_x)}} + \gamma\frac{1}{1+e^{\omega(\pi_x-\alpha)}}, \tag{10}$$

where the parameter $\omega \geqslant 0$ represents the selection intensity. The above process was repeated for the following time step. The Monte Carlo simulation procedure was also applied to obtain the dynamics of the MFC in the random-matching model.

III. RESULTS

A. Well-mixed population

This section discusses the evolutionary dynamics of the proposed model in a homogeneous mixed finite population. Taking the Prisoner's Dilemma as an example, Fig. 4. shows diagrams of the transition probabilities of different mixed models where the horizontal axis represents states of the proposed process. Except for the imitation process, all other transition probabilities in the mixed model decreased with state i of the system. It was also found that the transition probability of the mixed model increased with an increase in the γ value, that is, the transition probability of the imitation process ($\gamma = 0$) was always lower than that of other mixed processes, while that of the aspiration-driven process ($\gamma = 1$) was always higher than that of other processes.

In the context of a finite population with cognitive capabilities, the key concern related to the limit state of the population under the microscopic update mechanism. Consequently, the proposed model is not related to evolutionary time scales, but only to the state of the population at a certain moment. It should here be noted that, if $\gamma = 0$, the proposed process is the so-called imitation process, and the Markov chain expressed by Eqs. (6a)–(6c) is a birth–death process with absorbing states 0 and N. As a matter of convenience, only the case $\gamma \in (0, 1]$ was considered, where, as a result of the aspiration-driven dynamics, the evolutionary process expressed by Eqs. (6a)–(6c) denotes an ergodic Markov chain with reflecting boundaries. Therefore, the abundance of cooperators for the proposed mixed process was next calculated, instead of the fixation probability, which is the probability of being absorbed into one of the two states [33,52]. The mean abundance of cooperators reflects the limiting expected value of the proportion of the total number of cooperators.

If $q_t(j)$ describes the probability that the system is found in state j at time t, then the master equation of $q_t(j)$ is

$$\begin{aligned} q_{t+1}(j) = {} & q_t(j-1)p_{j-1,j} + q_t(j+1)p_{j+1,j} \\ & + q_t(j)(1 - p_{j,j+1} - p_{j,j-1}). \end{aligned} \tag{11}$$

According to the properties of the ergodic Markov chain, there is a unique stationary probability distribution, $\psi = (\psi_0, \psi_1, \cdots, \psi_j, \cdots, \psi_N)$, over the abundance of C, where

$$\lim_{t\to\infty} q_t(j) = \psi_j. \tag{12}$$

Whereby ψ_j satisfies the balance equation [30]

$$\psi_j = p_{i+1,i}\psi_{j+1} + p_{i-1,i}\psi_{j-1} + (1 - p_{i,i+1} - p_{i,i-1})\psi_j. \tag{13}$$

Then, Eq. (13) satisfies the detailed balance condition [53]

$$\begin{aligned} \sum_{j=0}^{N} \psi_j &= 1, \\ \psi_{j-1}P_{j-1,j} &= \psi_j P_{j,j-1}. \end{aligned} \tag{14}$$

Equation (14) was then rearranged to

$$\psi_j = \frac{P_{j-1,j}}{P_{j,j-1}}\psi_{j-1}. \tag{15}$$

Therefore,

$$\psi_1 = \frac{P_{0,1}}{P_{1,0}}\psi_0, \tag{16}$$

$$\psi_2 = \frac{P_{1,2}}{P_{2,1}}\psi_1 = \frac{P_{0,1}}{P_{1,0}}\frac{P_{1,2}}{P_{2,1}}\psi_0, \tag{17}$$

$$\psi_3 = \frac{P_{2,3}}{P_{3,2}}\psi_2 = \frac{P_{0,1}}{P_{1,0}}\frac{P_{1,2}}{P_{2,1}}\frac{P_{2,3}}{P_{3,2}}\psi_0. \tag{18}$$

Then,

$$\psi_j = \frac{P_{0,1}}{P_{j,j-1}}\prod_{i=1}^{j-1}\frac{P_{i,i+1}}{P_{i,i-1}}\psi_0,\ 1 \leqslant j \leqslant N. \tag{19}$$

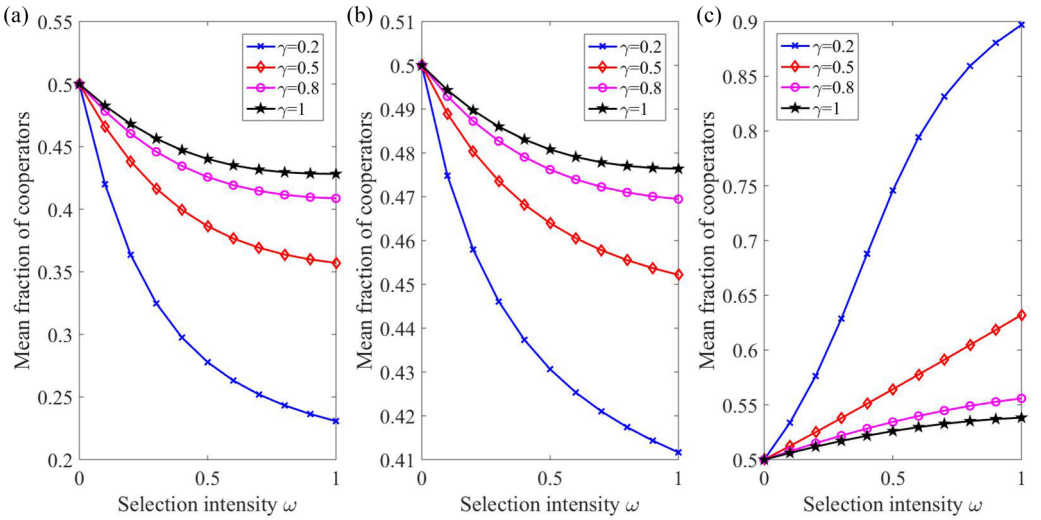

FIG. 5. The MFC results vary in accordance with the selection intensity, ω, for three games, where $\alpha = 4$ and $N = 100$. Panel (a) depicts the MFC in the Prisoner's Dilemma game, where $R = 3$, $S = 1$, $T = 5$, and $P = 2$. Panel (b) depicts the MFC in the coexistence game, where $R = 3$, $S = 2$, $T = 5$, and $P = 1$. Panel (c) depicts the MFC in the coordination game, where $R = 5$, $S = 1$, $T = 3$, and $P = 2$. The blue crosses, red diamonds, magenta circles, and black pentagrams show the proposed processes, these being $\gamma = 0.2$, $\gamma = 0.5$, $\gamma = 0.8$, and $\gamma = 1$, respectively.

However, $\sum_{j=0}^{N} \psi_j = 1$, thus yielding the following:

$$\sum_{j=0}^{N} \psi_j = \psi_0 \left(1 + \sum_{j=1}^{N} \frac{P_{0,1}}{P_{j,j-1}} \prod_{i=1}^{j-1} \frac{P_{i,i+1}}{P_{i,i-1}} \right) = 1. \tag{20}$$

Hence,

$$\psi_0 = \frac{1}{1 + \sum_{j=1}^{N} \frac{P_{0,1}}{P_{j,j-1}} \prod_{i=1}^{j-1} \frac{P_{i,i+1}}{P_{i,i-1}}}. \tag{21}$$

Therefore, according to the above equations,

$$\psi_j = \frac{\frac{P_{0,1}}{P_{j,j-1}} \prod_{i=1}^{j-1} \frac{P_{i,i+1}}{P_{i,i-1}}}{1 + \sum_{k=1}^{N} \frac{P_{0,1}}{P_{k,k-1}} \prod_{i=1}^{k-1} \frac{P_{i,i+1}}{P_{i,i-1}}}. \tag{22}$$

Then, the exact solution can be found by recursion:

$$\psi_j = \begin{cases} \frac{1}{1+\sum_{j=1}^{N} \frac{P_{0,1}}{P_{j,j-1}} \prod_{i=1}^{j-1} \frac{P_{i,i+1}}{P_{i,i-1}}}, & j = 0 \\ \frac{\frac{P_{0,1}}{P_{j,j-1}} \prod_{i=1}^{j-1} \frac{P_{i,i+1}}{P_{i,i-1}}}{1+\sum_{k=1}^{N} \frac{P_{0,1}}{P_{k,k-1}} \prod_{i=1}^{k-1} \frac{P_{i,i+1}}{P_{i,i-1}}}, & 1 \leqslant j \leqslant N \end{cases}. \tag{23}$$

X_C is defined as the abundance of cooperators of the proposed mixed process. Then, the exact value of X_C can be defined as

$$X_C = \sum_{j=0}^{N} \frac{j}{N} \psi_j. \tag{24}$$

Equation (24) also represents the average abundance of cooperators over all possible states, i.e., MFC. For the proposed model, this calculation was deemed too complicated for deriving the specific analytical results. As such, numerical calculation was taken as a powerful tool, because this can obtain the relationships between the mean fraction of the cooperators and the selection intensity ω, probability γ, and aspiration level α.

Figure 5 shows the change of MFC with respect to selection intensity, ω, under the various mixed updating processes ($\gamma = 0.2, 0.5, 0.8$). Figures 5(a)–5(c) represent the Prisoner's Dilemma, coexistence, and coordination games, respectively. In the first two games, the MFC can be seen to decrease as the selection intensity, ω, increases. The smaller the value of γ, the higher the rate at which MFC decreases with ω. However, in the coordination game, the MFC increases with the selection intensity, ω. The smaller the value of γ, the higher the rate at which MFC increases with ω. From Fig. 5, the conclusion can also be drawn that the aspiration-driven update rule greatly promotes cooperation in the Prisoner's Dilemma and coexistence games, but inhibits it in the coordination game.

Changes of the MFC were simulated with γ. The results are shown in Fig. 6(a). The MFC in the Prisoner's Dilemma and coexistence games increases as γ increases, whereas it decreases in the coordination game. The rate of change in the MFC is larger with γ for the coordination game than for the Prisoner's Dilemma and coexistence games. In Fig. 6(b), the Prisoner's Dilemma can be seen to have the highest MFC, whereas the coordination game has the lowest. As the aspiration level α increases, the MFC decreases in these two games, but increases in the coexistence game. When the level of aspiration exceeds the maximum of the payoff matrix, i.e., $\alpha > 5$, the MFC changes very slowly and then tends to stabilize.

B. Structured population

To further support the current claims, it was considered how the mixed update rule would affect the evolution of cooperation in spatially extended populations, such as square lattice, scale-free, and small-world networks. Given the computational difficulties of theoretical analysis, a simulation analysis was used to analyze the dynamic evolution of

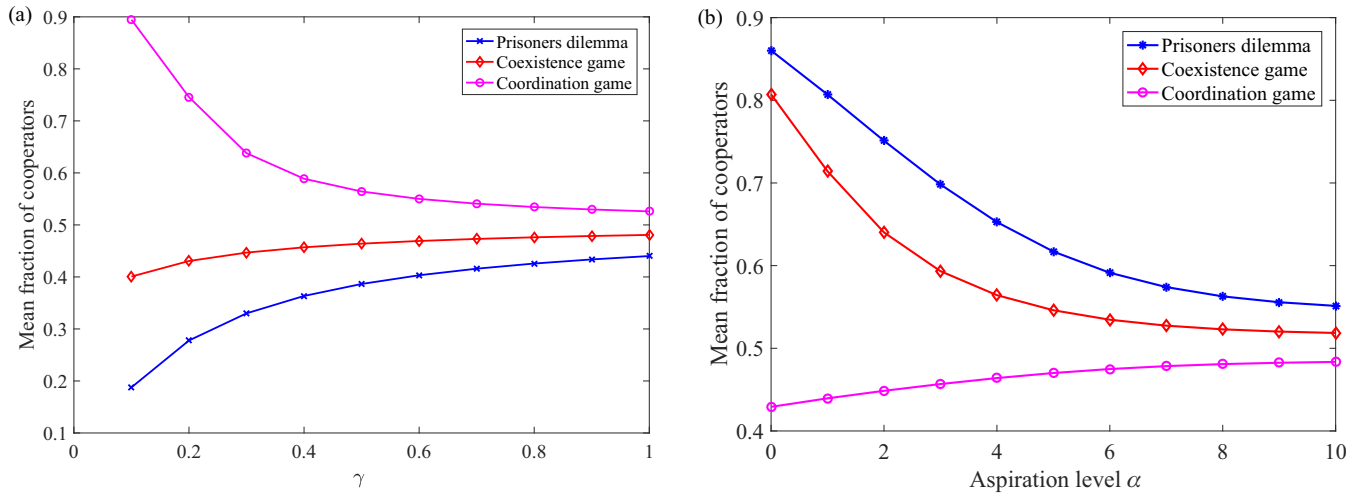

FIG. 6. MFC results in an unstructured population with $N = 100$ and $\omega = 0.5$. Panel (a) depicts the relationships between the MFC and γ, where $\alpha = 4$; panel (b) depicts the relationships between the MFC and α, where $\gamma = 0.5$. The blue stars, red diamonds, and magenta circles correspond to the Prisoner's Dilemma ($R = 3, S = 1, T = 5, P = 2$), coexistence game ($R = 3, S = 2, T = 5, P = 1$), and coordination game ($R = 5, S = 1, T = 3, P = 2$), respectively.

structured populations. The Monte Carlo simulation procedure was used to obtain the dynamics of cooperation in structured populations. The Monte Carlo dynamics were run until the network achieved a stable state, where the MFC fluctuated around a mean value. It should be noted that other sizes of structured populations can be also implemented in such a simulation, which does not affect the simulation results.

The asynchronous Monte Carlo procedure was applied to simulate the evolutionary dynamics. First, it was assumed that the players were confined to sites on a regular 100×100 square lattice with periodic boundary conditions. Each site contained one individual with two strategies, C and D. Then, the mean payoffs obtained from the games between an individual and their four nearest neighbors were taken as the payoffs of the individual. Each individual changed their strategy according to the imitation update rule with the probability $1 - \gamma$, or the aspiration-driven update rule with the probability γ, according to the transition probabilities [Eq. (8)]. Starting with a random initial state, where individuals randomly selected C or D, each simulation lasted until the population reached a stable state (10^5–2×10^5 rounds), and 30 simulations were run. The mean and standard deviations were taken over the last 10^4 rounds, and the simulation results averaged over 30 runs.

Figure 7 describes the relationship between the MFC and the selection intensity, ω, for the proposed model, with $\gamma = 0.2, 0.5, 0.8$ in the square lattice network. For the Prisoner's Dilemma and coexistence games, the MFC can be seen to increase with the selection intensity, ω, when $\gamma = 0.2, 0.5$. When $\gamma = 0.2$, the change rate of the MFC is greater than that when $\gamma = 0.5$. However, as $\gamma = 0.8, 1$, the MFC first decreases and then remains slightly altered with the selection intensity, ω. In the coordination game, the MFC increases with selection intensity, ω, as $\gamma = 0.5, 0.8, 1$. If $\gamma = 0.2$, then the MFC first increases and then decreases with the selection intensity ω, but this change is not obvious. Additionally, when $\gamma = 0.2$, the MFC is highest in the Prisoner's Dilemma and coexistence games, and smallest in the coordination game.

By comparing Fig. 7 to Fig. 5, it can be seen that in the Prisoner's Dilemma and coexistence games, the aspiration-driven update mechanism of the mixed process promotes cooperation in a well-mixed population, but inhibits cooperation in a square lattice network. In the coordination game, the effect of the aspiration-driven update mechanism is also different in both populations. For the three games, in a well-mixed population and with an increase in the value of γ value, the change rate of the MFC with selection intensity ω decreases. In addition, the MFC monotonously rises or declines with selection intensity ω in a well-mixed population, while this is not always the case in lattice networks. The behavior of the MFC in a square lattice is more complex than that in a well-mixed population.

Figure 8(a) states the relationship between the MFC and in the square lattice. In the Prisoner's Dilemma and coexistence games, the MFC decreases with γ. A smaller value of γ results in a higher rate of decrease. However, in the coordination game, the MFC increases with γ. The MFC change trends in the three games run contrary to those in homogeneous populations [Fig. 6(a)]. The aspiration-driven process plays a different role in the well-mixed populations and square lattice, i.e., it promotes cooperation in homogeneous populations, but inhibits the cooperation of square lattice networks in the Prisoner's Dilemma and coexistence games. However, interestingly, the process inhibits cooperation in homogeneous populations, but promotes cooperation in square lattice networks in the coordination game.

The individual's aspiration level, α, represents the individual's degree of satisfaction with the current game payoff and directly determines if the individual is willing to change their current strategy. Figure 8(b) depicts the effect of α on MFC, where a phase transition point, $\alpha \approx 3$, can be seen. When the level of aspiration is lower than 3, the MFC decreases with the aspiration level α in the Prisoner's Dilemma and coexistence games and increases in the coordination game. However, if the aspiration level is greater than 3 but less than 5, then the MFC in the Prisoner's Dilemma and coexistence

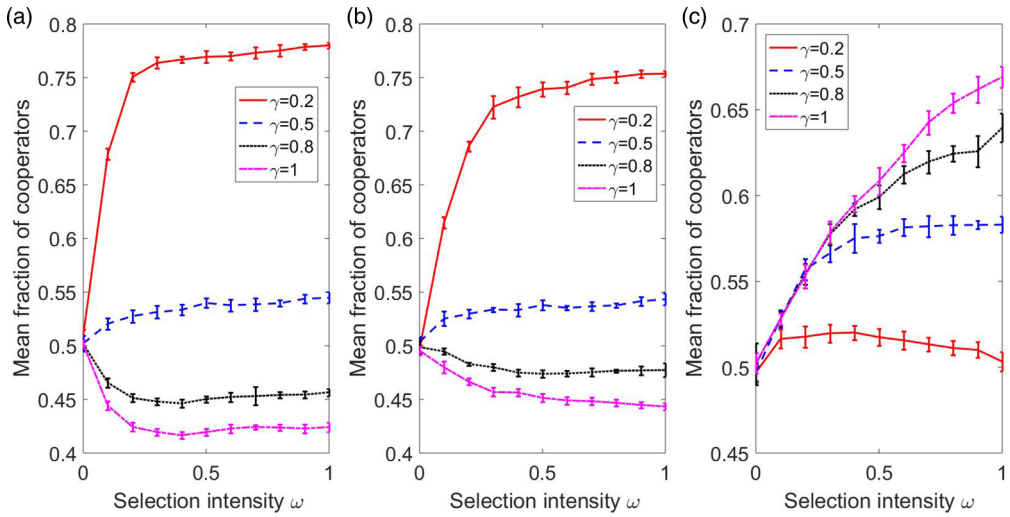

FIG. 7. The MFC varies with the selection intensity ω, in the three games with $N = 100 \times 100$ and $\alpha = 4$: (a) in the Prisoner's Dilemma with $R = 3$, $S = 1$, $T = 5$, and $P = 2$; (b) in the coexistence game with $R = 3$, $S = 2$, $T = 5$, and $P = 1$; (c) in the coordination game with $R = 5$, $S = 1$, $T = 3$, and $P = 2$. The red solid lines, blue dash lines, black dotted lines, and magenta dash-dotted lines show the proposed processes, with $\gamma = 0.2$, $\gamma = 0.5$, $\gamma = 0.8$, and $\gamma = 1$, respectively.

games increases, while decreasing in the coordination game. Furthermore, when the level of aspiration is greater than 5, the MFC remains basically unchanged across the three games.

To further support the current claims and better understand this phenomenon on a microscopic level, the snapshots of the square lattice in three games were analyzed (Fig. 9). According to Figs. 9(a) and 9(b), in the Prisoner's Dilemma, if $\gamma = 0.2$, the cooperators are found to be in a group; as γ goes up to 0.8, the cooperators' islands are destroyed by defectors. Consequently, from Figs. 8(a) and 9(a), 9(b), it can be concluded that the aspiration-driven rule inhibits cooperation in the square lattice. As can be seen from Figs. 9(c), 9(d), if $\gamma = 0.2$ in the coexistence game, then the cooperators are found to be in a group, but when γ goes up to 0.8, the cooperators' islands are also destroyed by defectors. In Figs. 8(a) and 9(c), 9(d), the aspiration-driven rule in the coexistence game is seen to inhibit cooperation in the square lattice network. Figures 9(e) and 9(f) demonstrate that, in the coordination game, the aspiration-driven rule promotes cooperation in the square lattice as γ increases. In short, in the square lattice, Figs. 8(a) and 9 demonstrate that the aspiration-driven rule promotes cooperation in the first two games, and inhibits cooperation in the last one.

Well-mixed populations and square lattice networks can be regarded as regular networks. However, most networks in the real world are not regular. Two more realistic network structures are the small-world networks proposed by Watts and Strogatz [54] in 1998, and scale-free networks proposed by Barabási and Albert [55] in 1999. The small-world network,

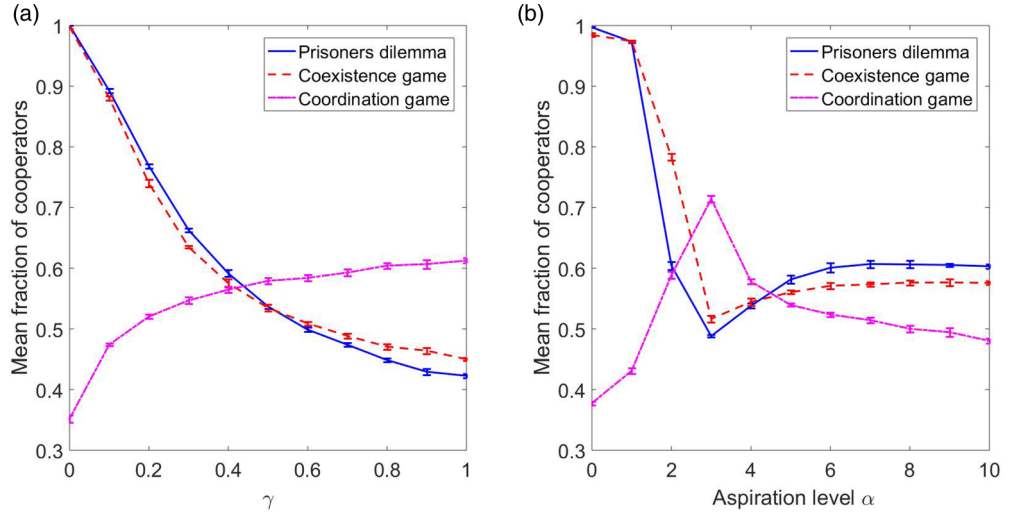

FIG. 8. In the 100×100 square lattice, MFC versus the probability γ in panel (a), where $\omega = 0.5$ and $\alpha = 4$, and MFC versus the individuals' aspiration level α in panel (b), where $\omega = 0.5$ and $\gamma = 0.5$. The blue solid lines, red dash lines, and magenta dash-dotted lines represent the Prisoner's Dilemma ($R = 3$, $S = 1$, $T = 5$, and $P = 2$), coexistence game ($R = 3$, $S = 2$, $T = 5$, and $P = 1$), and coordination game ($R = 5$, $S = 1$, $T = 3$, and $P = 2$), respectively.

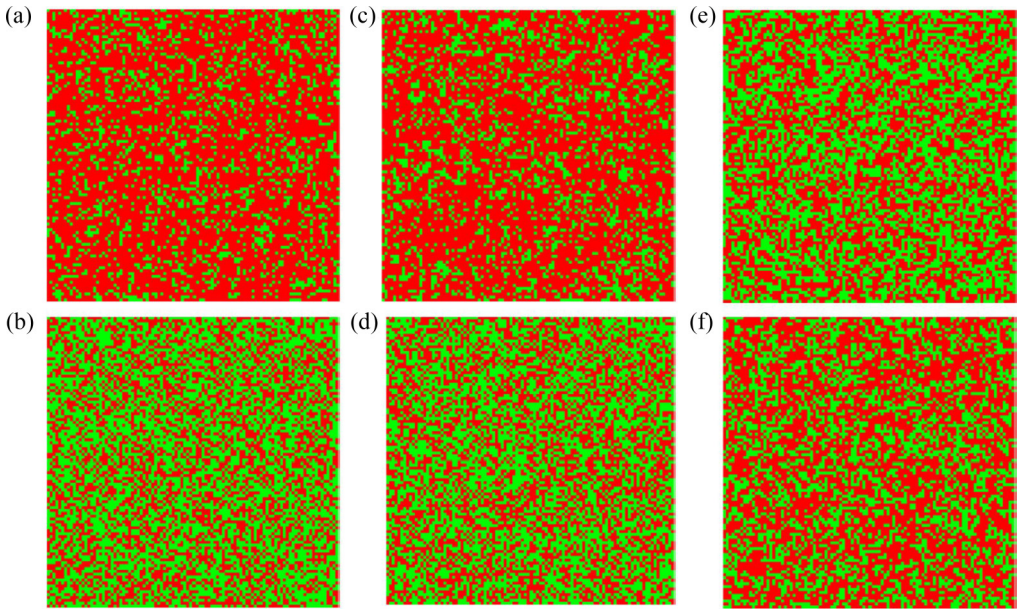

FIG. 9. Snapshots of the 100 × 100 square lattice in the three games with $\omega = 0.1$. The figure shows the results of: (a), (b) Prisoner's Dilemma with $R = 3$, $S = 1$, $T = 5$, and $P = 2$; (c), (d) coexistence game with $R = 3$, $S = 2$, $T = 5$, and $P = 1$; (e), (f) coordination game with $R = 5$, $S = 1$, $T = 3$, and $P = 2$. $\gamma = 0.2$ for (a), (c), (e) and $\gamma = 0.8$ for (b), (d), (f). Cooperators are depicted in red and defectors in green.

in which most nodes are not adjacent to each other but can be connected via a small number of hops, exists in mathematics, physics, and sociology, and is a mathematical graph model. A complex network whose degree distribution conforms to the power law distribution is a scale-free network, i.e., only a few nodes tend to have a large number of connections. In both structural networks, the MFC was analyzed according to the proposed hybrid update process by using a simulation analysis. The results are shown in Figs. 10 and 11.

For the scale-free network, it was assumed that the size $N = 10000$. At the initial time, a complete network with $m_0 = 20$ nodes was established. Then, at each time step, a new node was added and connected to $m = 5$ of the initial $m_0 = 20$ nodes. The above process was repeated until the number of nodes increased to 10 000. For the small-world network, a regular circular network was assumed, with $N = 10000$ nodes, each of which was connected by $K = 6$ edges to the six nearest neighboring nodes. Then, an edge was added between a randomly selected pair of nodes with a probability of 0.5. Any two different nodes could have only one edge at most, and each node could not be connected to itself. The simulation lasted until the population reached a stable state

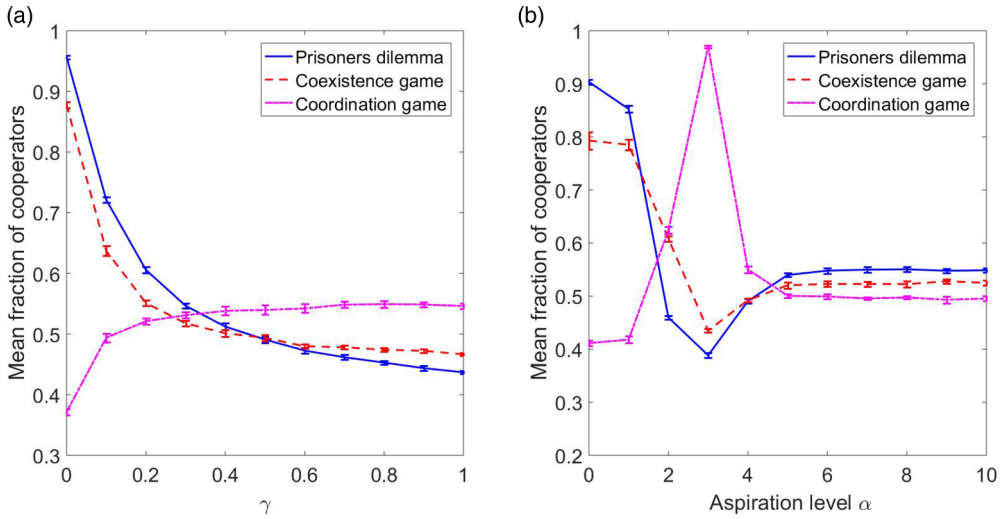

FIG. 10. In a scale-free network of size $N = 10000$, panel (a) shows the MFC versus the probability γ, where $\omega = 0.5$ and $\alpha = 4$; panel (b) shows the MFC versus the individuals' aspiration level α, where $\omega = 0.5$ and $\gamma = 0.5$. The blue solid lines, red dash lines, and magenta dash-dotted lines represent the Prisoner's Dilemma ($R = 3$, $S = 1$, $T = 5$, and $P = 2$), coexistence game ($R = 3$, $S = 2$, $T = 5$, and $P = 1$), and coordination game ($R = 5$, $S = 1$, $T = 3$, and $P = 2$), respectively.

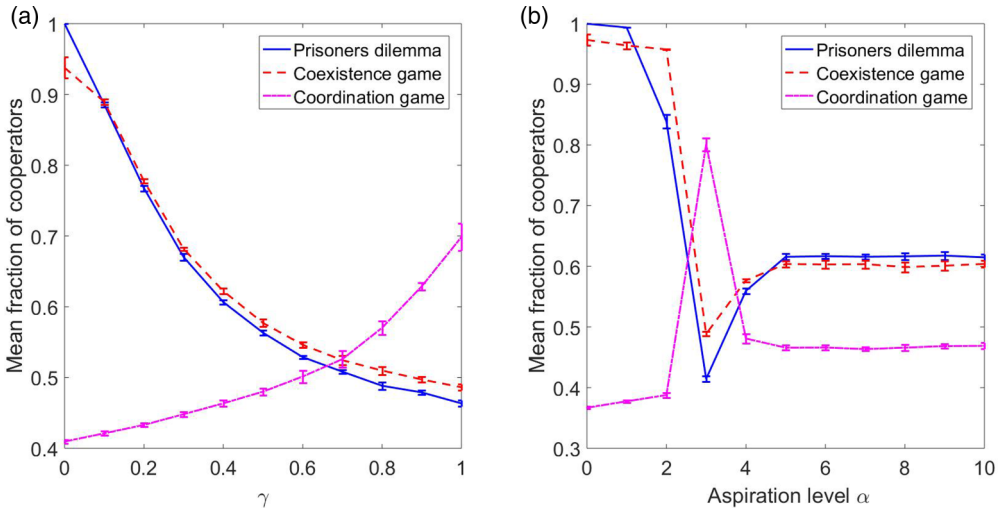

FIG. 11. In a small-world network of size $N = 10000$, panel (a) shows the MFC versus the probability γ, where $\omega = 0.5$ and $\alpha = 4$; panel (b) shows the MFC versus the individuals' aspiration level α, where $\omega = 0.5$ and $\gamma = 0.5$. The blue solid lines, red dash lines, and magenta dash-dotted lines represent the Prisoner's Dilemma ($R = 3$, $S = 1$, $T = 5$, and $P = 2$), coexistence game ($R = 3$, $S = 2$, $T = 5$, and $P = 1$), and coordination game ($R = 5$, $S = 1$, $T = 3$, and $P = 2$), respectively.

(about 10^5–2×10^5 rounds). Thus, it was determined that each simulation ran for 2×10^5 rounds for each network, taking the mean and standard deviations over the last 10^4 rounds as the results. Starting with a random initial state, where individuals randomly selected C or D, 30 simulations were run. The simulation results are averaged over 30 simulations.

According to Figs. 10(a) and 11(a), in the scale-free and small-world networks of the Prisoner's Dilemma and coexistence games, the MFC decreases with γ, i.e., the aspiration-driven update rule inhibits cooperation. Conversely, for the coordination game, the MFC increases as γ decreases, i.e., the aspiration-driven update rule promotes cooperation. These results are consistent with those of the square lattice network, but inconsistent with those in homogeneous mixed populations. According to Figs. 10(b) and 11(b), in the Prisoner's Dilemma and coexistence games, the MFC first decreases and then increases with γ. However, in the coordination game, the MFC first increases and then decreases. The turning point appears at $\alpha \approx 3$ in the three games. When the level of aspiration is almost greater than $\alpha = 5$, the MFC tends to be stable. Compared to Figs. 6(b) and 8(b), it was found that the changes of MFC with the aspiration level in the square lattice, scale-free and small-world networks were more complex than those in the well-mixed populations.

C. Random-matching model

As an extension, this section discusses the evolutionary game dynamics of the random matching model based on

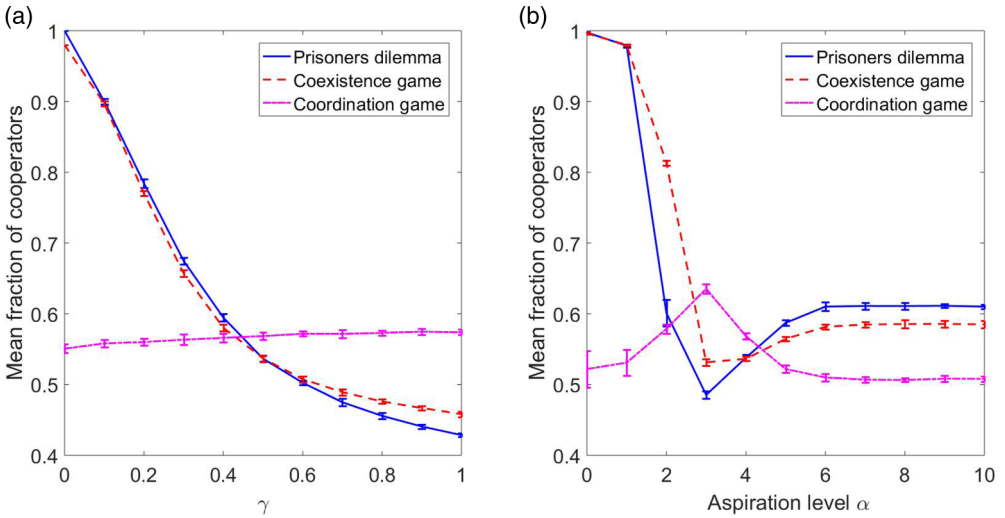

FIG. 12. In a random-matching model with size $N = 10000$, panel (a) shows the MFC versus the probability γ, where $\omega = 0.5$ and $\alpha = 4$; panel (b) shows the MFC versus the individuals' aspiration level α, where $\omega = 0.5$ and $\gamma = 0.5$. The blue solid lines, red dash lines, and magenta dash-dotted lines represent the Prisoner's Dilemma ($R = 3$, $S = 1$, $T = 5$, and $P = 2$), coexistence game ($R = 3$, $S = 2$, $T = 5$, and $P = 1$), and coordination game ($R = 5$, $S = 1$, $T = 3$, and $P = 2$), respectively. The standard deviation was applied as the error bar.

the neoteric update rule presented in this paper. In each time step, individuals were arranged on a random regular graph and interacted with their neighbors, whereby a focal individual updated its strategy through that of a randomly selected neighbor, or by comparing their payoffs to their aspiration level. Thus, an individual's fitness was stochastic, just as in structured populations [46]. The Monte Carlo simulation procedure was also applied to obtain the dynamics of cooperation in a random-matching model, thereafter comparing the results of the random-matching model with those of the homogeneous mixed population and square lattice networks.

Figure 12 presents the results of the random-matching model with degree $k = 4$ and size $N = 10000$. It also should be noted that the population size in the random matching model did not affect the simulation results. Here, it can be seen that for the random matching model, in the Prisoner's Dilemma and coexistence games, the MFC decreases with the increase of γ, while it increases with the increase of γ in the coordination game [Fig. 12(a)]. That is to say, with the increase of probability γ upon adopting the aspiration-driven update rule, the MFC keeps decreasing in the first two games, meaning that the aspiration-driven updating rule inhibits cooperation. This conclusion is consistent with that obtained from the analysis of the square lattice network [Fig. 8(a)]. Howerer, this differs from the results in the well-mixed population, as presented in Fig. 6(a). According to Fig. 12(b), in the Prisoner's Dilemma and coexistence games, the MFC first decreases and then increases with the level of aspiration, while in the coordination game, the MFC first increases and then decreases. Across the three games, the phase transition point is approximately $\alpha = 3$. When the level of aspiration is almost greater than $\alpha = 5$, the MFC also tends to be stable. The change rule is the same as that of the square lattice [Fig. 8(b)], except for the rate of change.

IV. CONCLUSION

Cooperation is a universal phenomenon that exists in many fields, such as human society and biological groups. The promotion of cooperation has always been an important issue in the evolutionary game. In finite populations, two fundamentally different mechanisms [32] can be used to classify strategy updating and population dynamics according to the knowledge that individuals possess about their strategic environment or themselves: to imitate others and self-learning in line with the individual's own aspiration. The most important difference with the aspiration-driven process is that it does not require any knowledge about the payoffs of other individuals; i.e., the aspiration-driven update dynamic, which is a form of self-learning, requires less information about an individual's strategic environment than do imitation dynamics. To date, the imitation and aspiration-driven processes have been broadly studied in various topologies for different games. However, the studies on evolutionary dynamics have concentrated on single update rules. The assumption that each individual in a population adopts a single update rule to shift their strategy is idealized and unrealistic. Therefore, the current study combined the imitation process with the aspiration-driven update process to establish a new mixed model. This model removes the assumption that an individual uses a single rule for updating their strategy and, therefore, differs from previous models.

The motivation for studying this hybrid model was to explore whether or not the new mixed update rule favored the formation of cooperation. Specifically, the variance of MFC alongside certain factors was investigated, such as selection intensity ω, the probability γ with which an individual adopts the aspiration-driven rule, and aspiration level α. We studied not only a homogeneous mixed population, but also a structural population and random matching model. The results of the random latter were consistent with those in the square lattice, but different from those in the homogeneous mixed population. In the Prisoner's Dilemma, coexistence and coordination games, the aspiration-driven update rule played different roles. In the Prisoner's Dilemma and coexistence games, the aspiration update mechanism promoted cooperation in well-mixed populations but inhibited it in structured ones and in the random-matching model. However, the opposite effects emerged in the coordination game. In the structural populations and random matching model, the MFC was seen to have the same change trend with the selection intensity ω, but with a different rate of change. In the structural populations and random matching model, the MFC changed with the aspiration level and there occurred a phase transition point. In the Prisoner's Dilemma and coexistence games, the MFC had a minimum value at the phase transition point, and a maximum value at the phase transition point in the coordination game. In the structural populations and random matching model, the population size did not affect changes in the MFC, including those of the phase transition.

The present investigation sheds some light on the complex dynamics in a well-mixed population, structured populations and random-matching model, and also highlights the role of aspiration-driven processes in evolutionary games. Therefore, the current work may be helpful in understanding the cooperative behavior induced by combining imitation and aspiration-driven update rules in the different population structures. Owing to the complexity and variability of the external environment and the internal sophistication of the individual, the tendency of individuals to change their strategies through mixed update rules is understandable, and in line with human psychology. Consequently, future studies should consider evolutionary dynamics combining more than two updating processes. Thus, it can also be expected that much more complicated dynamics would occur in the different contexts of network structure populations. In addition, individuals in a population are generally heterogeneous. The level of desire is not necessarily the same for each individual. Therefore, future studies could also consider the population dynamics caused by the heterogeneity of individual aspiration.

ACKNOWLEDGMENTS

The research was supported by the National Science Foundation of China (Grants No. 71871171, No. 71871173, and No. 71832010).

[1] M. A. Amaral, L. Wardil, M. Perc, and J. K. L. Da Silva, Phys. Rev. E **93**, 042304 (2016).

[2] J. Hofbauer and K. Sigmund, *Evolutionary Games and Population Dynamics* (Cambridge University Press, Cambridge, UK, 1998).

[3] M. Mestertongibbons, *An Introduction to Game-Theoretic Modelling* (AMS, Providence, RI, 2001).

[4] G. Szabó and C. Tőke, Phys. Rev. E **58**, 69 (1998).

[5] J. M. Smith, *Evolution and the Theory of Games* (Cambridge University Press, Cambridge, UK, 1982).

[6] K. R. Foster, T. Wenseleers, F. L. W. Ratnieks, and D. C. Queller, Trends Ecol. Evol. **21**, 599 (2006).

[7] K. Panchanathan and R. Boyd, Nature **432**, 499 (2015).

[8] D. Fundenberg and E. Maskin, Am. Econ. Rev. **80**, 274 (1990).

[9] A. Traulsen and M. A. Nowak, Proc. Natl. Acad. Sci. USA **103**, 10952 (2006).

[10] H. Ohtsuki and M. A. Nowak, J. Theor. Biol. **243**, 86 (2006).

[11] H. Ohtsuki and M. A. Nowak, J. Theor. Biol. **251**, 698 (2008).

[12] W. B. Du, X. B. Cao, M. B. Hu, and W. X. Wang, Europhys. Lett. **87**, 60004 (2009).

[13] P. D. Taylor and L. B. Jonker, Math. Biosci. **40**, 145 (1978).

[14] H. Gintis, *Game Theory Evolving* (Princeton University Press, Princeton, NJ, 2000).

[15] R. Cressman, *Evolutionary Dynamics and Extensive Form Games*, MIT Press Series on Economic Learning and Social Evolution (MIT Press, Cambridge, UK, 2003).

[16] J. C. Claussen and A. Traulsen, Phys. Rev. E **71**, 025101(R) (2005).

[17] L. A. Imhof, D. Fudenberg, and M. A. Nowak, Proc. Natl. Acad. Sci. USA **102**, 10797 (2005).

[18] M. A. Nowak and K. Sigmund, Science **303**, 793 (2004).

[19] D. Fudenberg, M. A. Nowak, C. Taylor, and L. A. Imhof, Theor. Popul. Biol. **70**, 352 (2006).

[20] M. E. Schaffer, J. Theor. Biol. **132**, 469 (1988).

[21] M. A. Nowak, A. Sasaki, C Taylor, and D. Fudenberg, Nature **428**, 646 (2004).

[22] P. A. P. Moran, *The Statistical Processes of Evolutionary Theory* (Clarendon Press, Oxford, 1962).

[23] P. M. Altrock and A. Traulsen, Phys. Rev. E **80**, 011909 (2009).

[24] M. A. Nowak, *Evolutionary Dynamics: Exploring the Equations of Life* (Harvard University Press, Cambridge, MA, 2006).

[25] A. Traulsen, J. M. Pacheco, and M. A. Nowak, J. Theor. Biol. **246**, 522 (2007).

[26] K. Sigmund, *The Calculus of Selfishness* (Princeton University Press, Princeton, NJ, 2010).

[27] A. Traulsen, J. C. Claussen, and C. Hauert, Phys. Rev. Lett. **95**, 238701 (2005).

[28] A. Traulsen, M. A. Nowak, and J. M. Pacheco, J. Theor. Biol. **244**, 349 (2007).

[29] P. M. Altrock and A. Traulsen, New J. Phys. **111**, 013012 (2009).

[30] X. S. Liu, M. F. He, Y. B. Kang, and Q. H. Pan, Physica A **484**, 336 (2017).

[31] J. M. Du, B. Wu, and L. Wang, Sci. Rep. **5**, 8014 (2015).

[32] J. M. Du, B. Wu, P. M. Altrock, and L. Wang, J. R. Soc. Interface **11**, 20140077 (2014).

[33] X. S. Liu, M. F. He, Y. B. Kang, and Q. H. Pan, Phys. Rev. E **94**, 012124 (2016).

[34] P. Matja and W. Zhen, PLoS ONE **5**, 515117 (2010).

[35] T. Platkowski, Appl. Math. Lett. **22**, 1161 (2009).

[36] T. Wu, F. Fu, and L. Wang, New J. Phys. **20**, 063007 (2018).

[37] X. Chen and L. Wang, Phys. Rev. E **77**, 017103 (2008).

[38] M. A. Amaral and M. A. Javarone, Phys. Rev. E **97**, 042305 (2018).

[39] X. S. Liu, Q. H. Pan, Y. B. Kang, and M. F. He, J. Theor. Biol. **364**, 242 (2015).

[40] X. S. Liu, Q. H. Pan, Y. B. Kang, and M. F. He, J. Theor. Biol. **387**, 214 (2015).

[41] J. L. Zhang, F. J. Weissing, and M. Cao, Phys. Rev. E **94**, 032407 (2016).

[42] X. J. Wang, C. L. Gu, S. J. Lv, and J. Quan, Chin. Phys. B **28**, 020203 (2019).

[43] C. Grüter, T. J. Czaczkes, and F. L. W. Ratnieks, Behav. Ecol. Sociobiol. **65**, 141 (2011).

[44] A. J. Robson and F. Vega-Redondo, J. Eco. Theor. **70**, 65 (1996).

[45] C. Hauert and J. Miękisz, Phys. Rev. E **98**, 052301 (2018).

[46] J. Miękisz, J. Theor. Biol **232**, 47 (2005).

[47] M. A. Amaral, M. Perc, L. Wardil, A. Szolnoki, E. J. da Silva Júnior, and J. K. L. da Silva, Phys. Rev. E **95**, 032307 (2017).

[48] L. A. Imhof and M. A. Nowak, J. Math. Biol. **52**, 667 (2006).

[49] P. Ashcroft, P. M. Altrock, and T. Galla, J. R. Soc. Interface **11**, 20140663 (2014).

[50] B. Wu, P. M. Altrock, L. Wang, and A. Traulsen, Phys. Rev. E **82**, 046106 (2010).

[51] Y. K. Liu, X. J. Chen, L. Wang, B. Li, W. G. Zhang, and H. F. Wang, Europhys. Lett. **94**, 60002 (2011).

[52] B. Wu, C. S. Gokhale, L. Wang, and A. Traulsen, J. Math. Biol. **64**, 803 (2012).

[53] N. G. V. Kampen, Phys. Today **36**, 78 (1983).

[54] D. J. Watts and S. H. Strogatz, Nature **393**, 440 (1998).

[55] A. L. Barabasi and R. Albert, Science **286**, 509 (1999).